Organic Process Research & Development **2010**, *14*, 840–848

The Synthesis of GV143253A: A Case Study for the Use of Analytical and Statistical Tools to Elucidate the Reaction Mechanism and to Optimize the Process

Giuseppe Guercio,*[,†] Alcide Perboni,[†] Francesco Tinazzi,[†] Luca Rovatti,[‡] and Stefano Provera[‡]

Chemical Development and Analytical Chemistry, GlaxoSmithKline Medicines Research Centre, Via Fleming 4, 37135, Verona, Italy

Abstract:

GV143253A 1 is a broad-spectrum injectable β-lactam belonging to the class of trinem antibiotics. This article describes the work which enabled a detailed process understanding via several analytical techniques and the subsequent optimization of a key intermediate. By means of a combined application of ^{31}P NMR spectroscopy and MS spectrometry, the main impurities have been identified and the reaction mechanisms clarified. Moreover, a design of experiments (DoE) approach was applied which substantially improved the overall yield.

1. Introduction

In recent years, bacteria have enhanced their mechanism of resistance to the most common antibacterial drugs. In particular, Methicillin-resistant *Staphylococcus aureus* (MRSA) represents one of the most challenging and threatening diseases globally.[1,2]

Among the various compounds screened, exomethylenyl trinem **1**[3] has emerged as a very potent anti-Gram positive agent with a remarkable activity against MRSA and also against some important Gram negative pathogens.

In this contribution we describe the success of efforts made with the aim of understanding the reaction mechanisms of two critical steps to improve the synthetic route for large-scale manufacturing. In particular, reaction monitoring was performed in real time using both ^{31}P NMR spectroscopy and MS spectrometry. The output of these studies was combined with a statistical tool in order to achieve a process improvement ensuring an appropriate scalability for the production of clinical batches.

2. Synthesis

The original synthesis of **1** was a linear process starting from the commercially available 4-acetoxyazetidinone. This synthetic approach was not ideal for further scale-up, as all of the intermediates possessed physical properties that were unsuitable for purification (e.g. by using standard crystallisation techniques). Our group developed an alternative route[4] which has been used for the synthesis of about 100 g of **1** (Scheme 1).

However, all synthetic steps suffered from low yields and nonreproducible reaction conditions. In particular, stage 2 was the most troublesome with a yield of ~33%. In this step β-enoneazetidinone **4** was converted, using a suitable oxalyl chloride **5**, into the oxalimide **6** (step 2a) that reacted with the diethoxymethylphosphine without isolation to afford the unstable and again nonisolable phosphorane intermediate **7** that was finally cyclized (step 2b) at higher temperature to give the desired compound **8**. To reach an acceptable cost of goods for **1**, the required target yield for this stage was ~60%. In order to achieve this, we initiated a thorough mechanistic investigation.

3. Design of Experiment (DoE) Study on Step 2a

The synthesis of the oxalimide[5] **6** was originally conducted using 2.0 equiv of FmOCOCOCl **5** and 2.2 equiv of *N,N*-diisopropylethylamine (DIPEA) with a typical yield of 45−50%. The conditions were optimized using a statistical approach coupled to a parallel equipment[6] (DoE, see Figure 1) to come up with an increased yield of 90−95% when changing the stoichiometry slightly (1.5 equiv of **5** and 2.0 equiv of DIPEA).

4. Analytical Techniques for the Elucidation of Step 2b

The literature-suggested mechanism for step 2b, the phosphorane formation **7** and its cyclization to **8**, is depicted in Scheme 2.[7] The first equivalent of diethoxymethylphosphine deoxygenates **6** to form a phosphine oxide and the highly reactive carbene **10** which is readily trapped by a second equivalent of the phosphine to form the phosphorane **7**. This unstable intermediate spontaneously cyclizes at higher temperature, leading to the desired **8** plus a second equivalent of phosphinoxide as a classical Wittig reaction.

The optimization of this synthetic step in the same way as was done for the oxalimide formation failed. All the studied parameters, e.g., temperature, equivalents of phosphine, solvents, etc., did not give the desired outcome, the solution yield being always lower than 50% and the isolated yield lower than 45%.

* To whom correspondence should be addressed. E-mail: giuseppe.2.guercio@gsk.com.

† Chemical Development.

‡ Analytical Chemistry.

(1) Klevens, R. M.; Morrison, M. A.; Nadle, J.; Petit, S.; Gershrnan, K.; Ray, S.; Harrison, L. H.; Lynfield, R.; Dumyati, G.; Townes, J. M.; Craig, A. S.; Zell, E. R.; Fosheim, G. E.; Mcdougal, L. K.; Carey, R. B.; Fridkin, S. K. *JAMA* **2007**, *298* (15), 1763.

(2) Klein, E.; Smith, D. L.; Laxminarayan, R. *Emerging Infect. Dis.* **2007**, *13* (12), 1840.

(3) Rossi, T.; Andreotti, D.; Tedesco, G.; Tarsi, L.; Ratti, E.; Feriani, A.; Pizzi, D. A.; Gaviraghi, G.; Biondi, S.; Finizia, G. *PCT Int. Appl.* **1998**, 9821210.

(4) Maragni, P.; Mattioli, M.; Pachera, R.; Perboni, A.; Tamburini, B. *Org. Process Res. Dev.* **2002**, *6*, 597.

(5) Plantan, I.; Selic, L.; Mesar, T.; Stefanic, A. P.; Oblak, M.; Prezelj, A.; Hesse, L.; Andrejasic, M.; Vilar, M.; Turk, D.; Kocijan, A.; Prevec, T.; Vilfan, G.; Kocjan, D.; Copar, A.; Urleb, U.; Solmajer, T. *J. Med. Chem.* **2007**, *50* (17), 4113.

(6) The software used for the statistical analysis was Design Expert DX 5. A central composite design (10 experiments with two central points) was performed considering FmOCOCOCl and DIPEA equivalents. The parallel equipment used was SK233 - Anachem.

(7) Battistini, C.; Scarafile, C.; Foglio, M.; Franceschi, G. *Tetrahedron Lett.* **1984**, *25* (22), 2395, and references therein.

Published on Web 06/08/2010

10.1021/op100097c

Scheme 1. **Initial overall process**

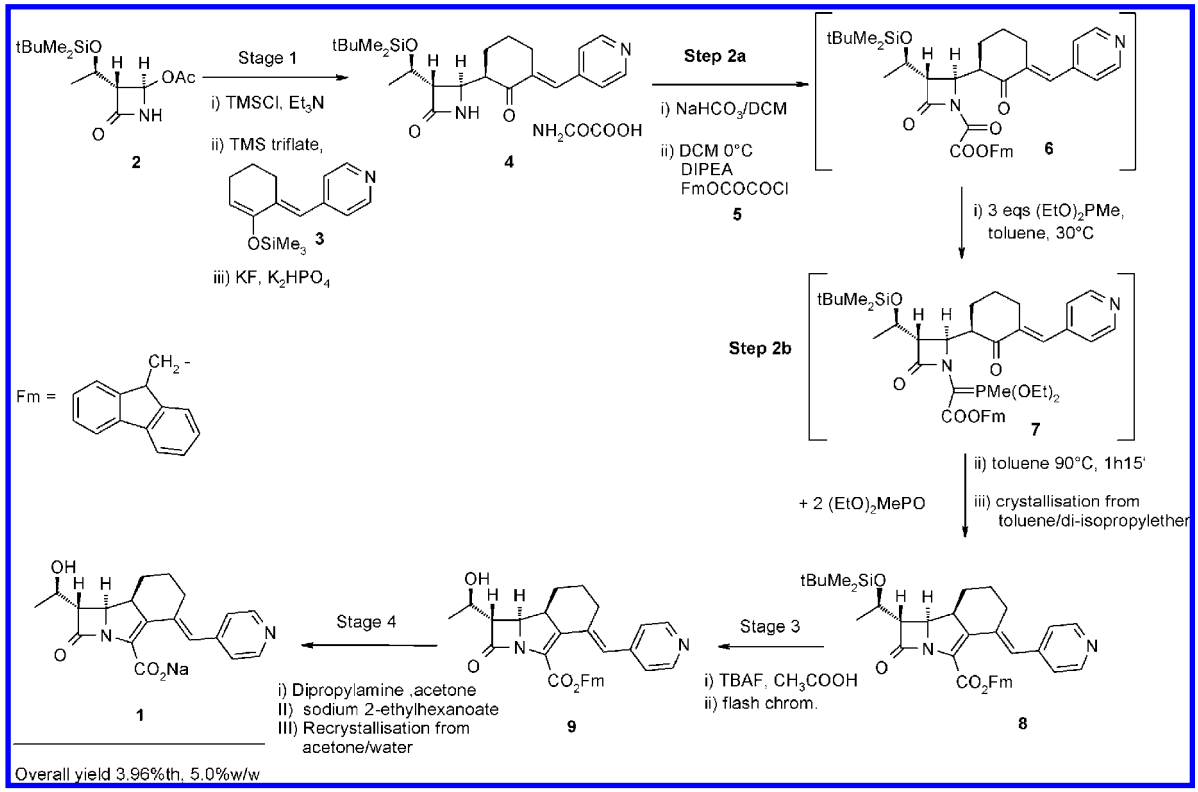

Moreover, no impurities were identified using a UV detector coupled to an isocratic HPLC system.

A different approach to this step was needed; in particular, the understanding of the reaction mechanism was required via the identification of the side products by means of different analytical techniques. The probe of a MS spectrometer was connected directly to a reactor to check the "in process" molecular weight of the products of the reactions. Moreover, some reactions were performed in a NMR tube checking the ^{31}P signals during the reaction in order to understand the nature and the relative amounts of the obtained intermediates containing phosphorous and their conversion to the final compound (the ^{1}H and ^{13}C signals were too complicated to be of use due to the presence of conformers, side products, and diastereoisomers in mixture).

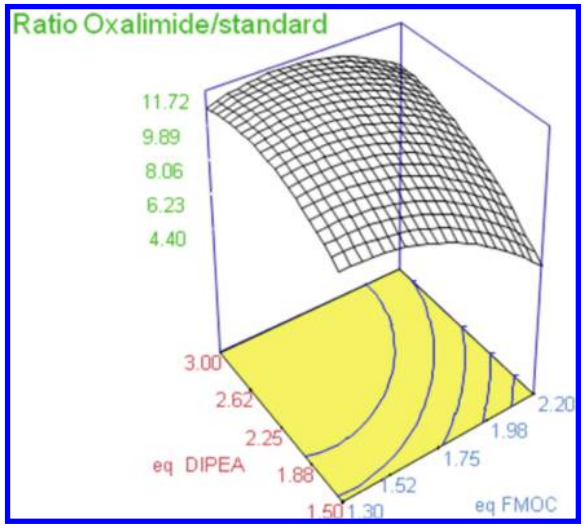

Figure 1. **Oxalimide optimization via DoE.**

4.1. MS Data. The reactions were performed both in toluene and in chloroform (the literature-suggested solvents) and monitored by MS spectrometry using ad hoc equipment and the procedure as described in the Experimental Section.

All the MS signals are associated with the species $[M + H]^+$ due to the positive electrospray ionization mode used. Regarding the reaction performed in toluene: (a) the signal at *m*/*z* 665 is associated with the protonated starting oxalimide **6**; (b) the signal at *m*/*z* 785 is associated with the desired phosphorane **7**, formed quickly in the first minutes; (c) the MS signal at *m*/*z* 893 was tentatively attributed to an impurity resulting from the addition of a second equivalent of phosphine to the phosphorane intermediate and subsequent loss of ethylene; (d) three other signals were also observed at *m*/*z* values of 801, 773, and 727, respectively. The signal at *m*/*z* 727 was attributed to the loss of ethanol from the species *m*/*z* 773 and the latter to the loss of ethylene from the species *m*/*z* 801 (Figure 2a).

The MS spectra obtained from the reaction performed in chloroform (Figure 2b) contained the same ion signals observed using toluene even if at different levels plus a number of new minor peaks. These observations suggested that the reactions are solvent dependent and chloroform does not seem to be the best solvent for the first part of the reaction.

At the end of the intermediate formation phase (about 60 min) the temperature of the reaction vessel was raised to 70 °C, and the cyclization to the desired compound **8** (*m*/*z* 633) started. Figure 3 gives the MS spectra obtained at the end of the reaction, and the following observations can be highlighted: (a) *m*/*z* 633 is a major peak in both spectra as well as *m*/*z* 785 and *m*/*z* 893; (b) the spectra

Scheme 2. **Step 2b literature-suggested mechanism**

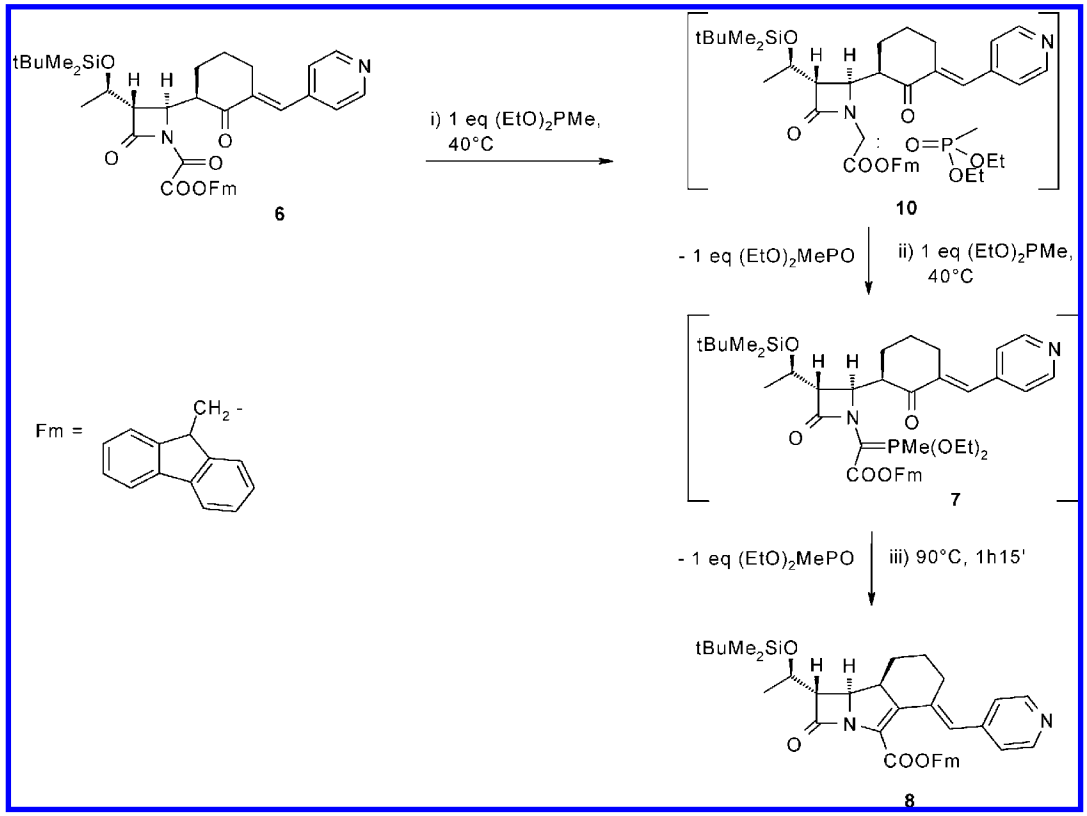

obtained in toluene contained also a major signal at *m*/*z* 847, tentatively attributed to the loss of ethanol from *m*/*z* 893; (c) other minor peaks were present at different levels in both spectra, among them, it is worth underlining the signal *m*/*z* 757 (loss of ethylene from the phosphorane **7**) and the signal *m*/*z* 769 associated with an adduct formed into an MS ion source [**8** + $(EtO)_2PMe$ + H]$^+$.

A kinetic reaction profile was finally obtained by reporting the relative intensities of the main MS signals as a function of the reaction time. The initial fast decrease of the signal associated with the starting oxalimide **6** was accompanied with a fast increase of the signal associated with the phosphorane **7**. Then, when the reaction mixture was heated, the cyclic **8** started forming with the simultaneous disappearance of the phospho-

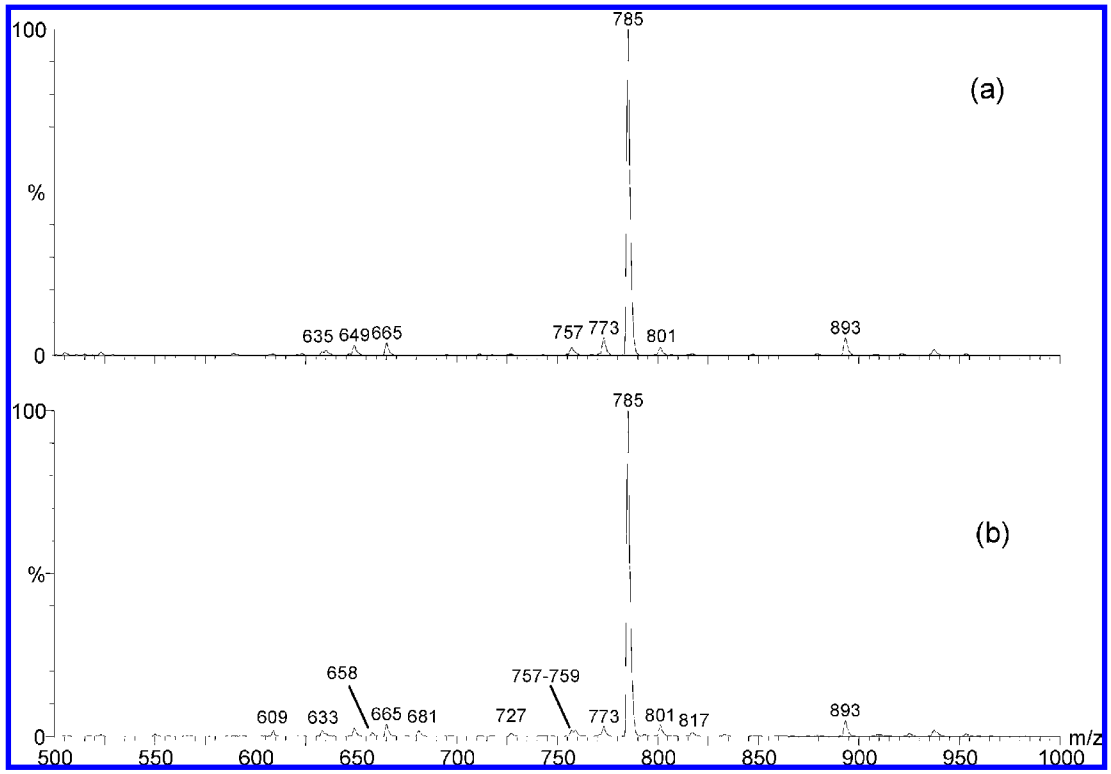

Figure 2. **MS spectra obtained at the end of the phosphorane formation performed in toluene (a) and in chloroform (b).**

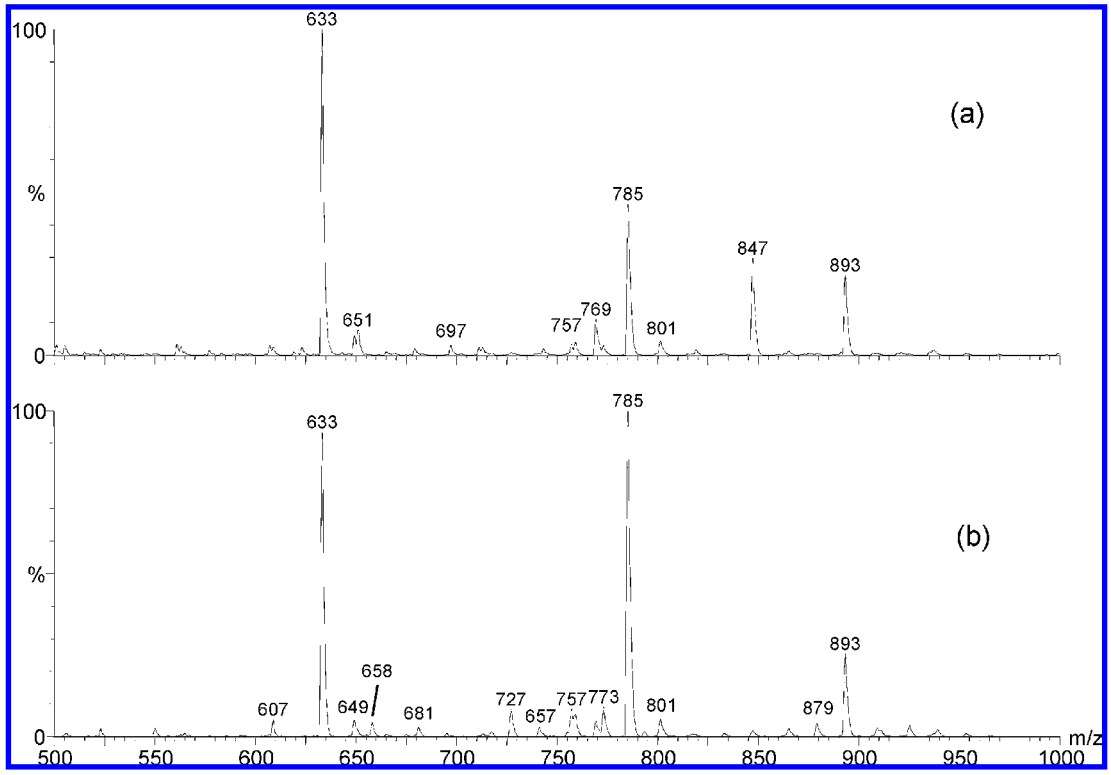

Figure 3. **MS analysis of cyclization performed in toluene (a) and in chloroform (b).**

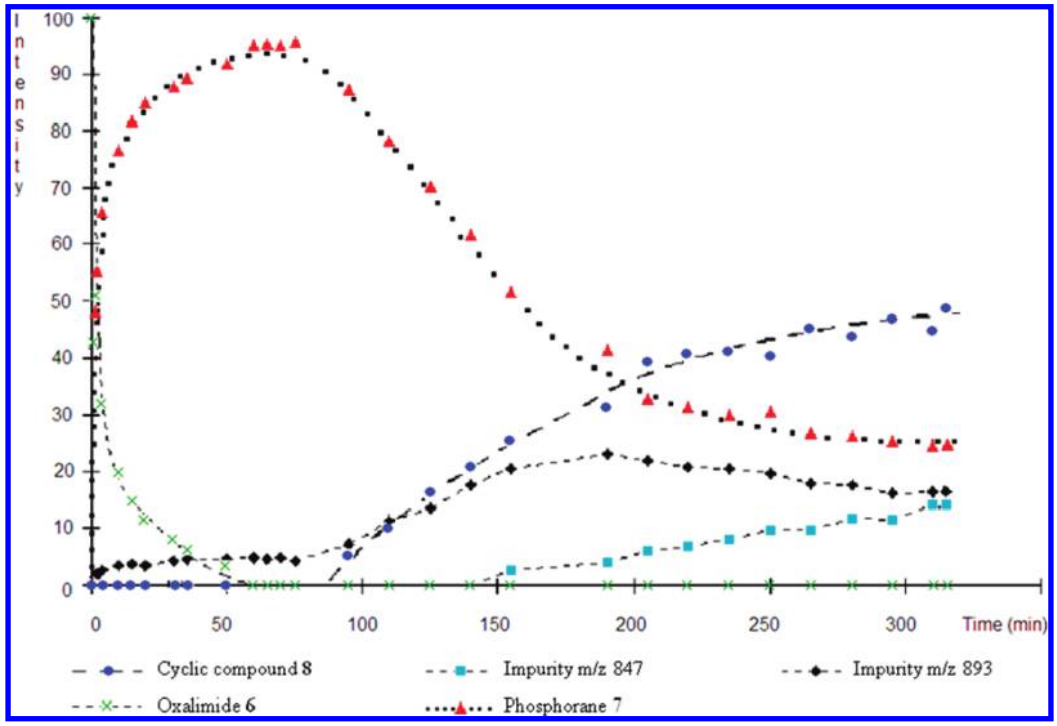

Figure 4. **Kinetic profile in toluene.**

rane **7**, the initial formation of the impurity 893 and its decrease, while 847 increased (Figure 4).

4.2. ^{31}P NMR Investigation. NMR analyses were required in order to obtain structural information regarding these side products as well as quantitative data. The reactions were performed at different temperatures directly in the NMR tubes, using deuterated toluene and chloroform as reaction solvents, respectively.

Figure 5 shows the phosphorane **7** synthesis both in toluene and in chloroform. From left to right we could identify the unreacted phosphine (175 ppm), the phosphorane intermediate **7** (3−4 peaks due to different species in equilibrium in the region 74−75 ppm), a hydride (phosphine side product always present in the starting material, 28 ppm), the phosphinoxide (side product of the reaction, 27 ppm), and an impurity present in larger amounts in chloroform than in toluene. Its chemical

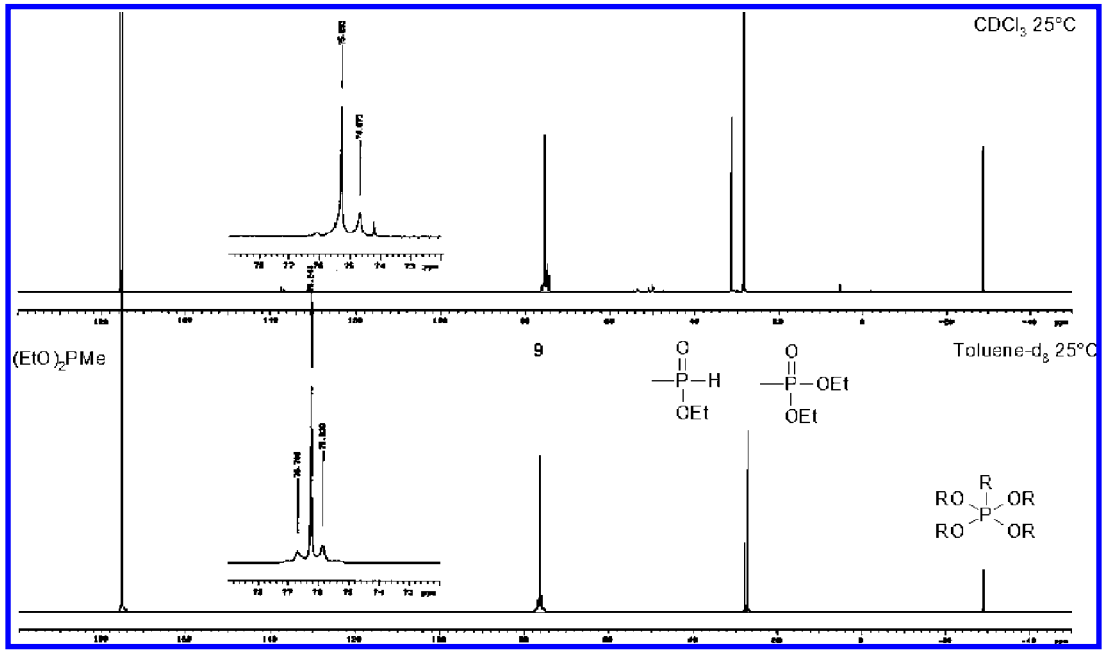

Figure 5. **NMR analysis of oxalimide formation performed in toluene and chloroform.**

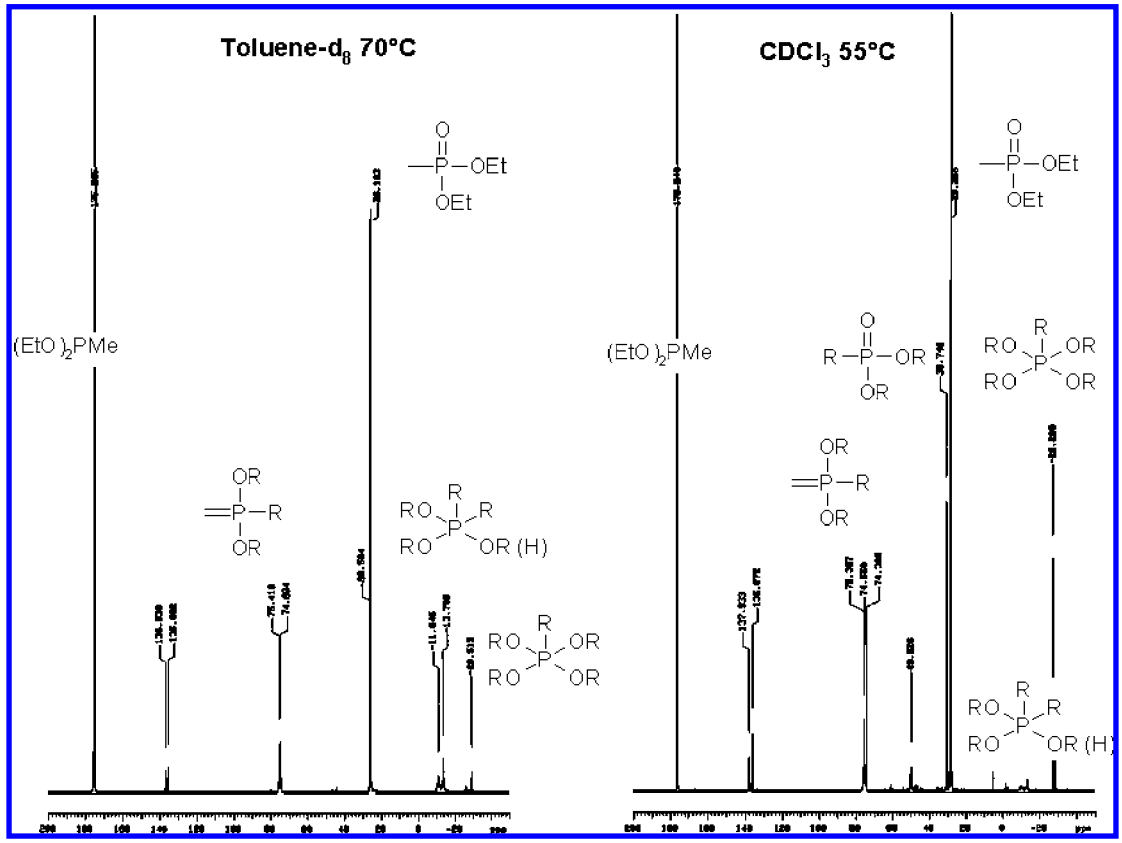

Figure 6. **NMR analysis of cyclization performed in toluene and chloroform.**

shift (−29 ppm) seems to suggest a penta-coordinated phosphorous tetraalkoxy-alkyl.

During the cyclization (Figure 6), apart from degradation peaks of the phosphine, the phosphorane **7** peak is decreasing due to its cyclization, but a signal remains at 75 ppm. This resonance could be still in agreement with phosphorus linked to a dialkoxy-alkyl-carbon double bond. Interestingly, this signal showed the same integration with the signal at −12/−13 ppm, suggesting the presence of a compound bearing another phosphorous in the same molecule, the second one being a pentavalent two-alkoxy-two-alkyl-hydroxyl. This species resulted in a larger amount in toluene with respect to that in chloroform. Moreover, the excess of integral at 76 ppm, phosphorane-like phosphorous, was balanced by the integration of the resonance at 51 ppm, suggesting the presence of a further molecule with two phosphorous atoms, the second one being coordinated to two-alkyl-alkoxy-oxygen double

Scheme 3. **Suggested structures and amount of the impurities**

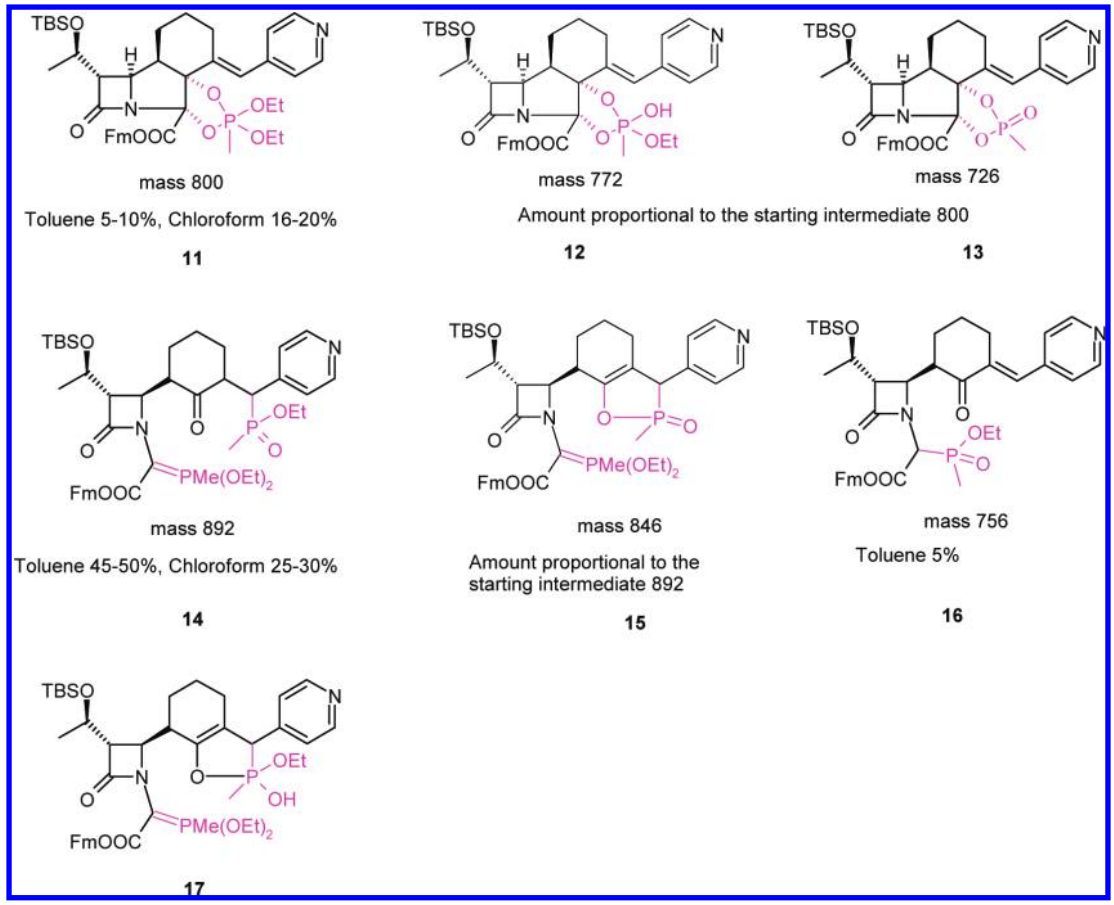

bond. Finally, the initially observed peak at −29 ppm was found again in relatively larger amounts in chloroform than in toluene.

4.3. Involved Intermediates and Proposed Mechanism. Having identified the mass of the major impurities and obtained some structural information by ^{31}P NMR chemical shifts as well as their relative amounts, it is possible to suggest the structures of all the species involved in the reaction (Scheme 3).

The peak *m*/*z* 801 can be associated with **11**, which would correspond to the phosphorus detected at −29 ppm in the NMR spectra, produced in a lower amount in toluene than in chloroform. **11** can lose ethylene, giving **12** (the *m*/*z* 773) and ethanol giving **13**[8] (the *m*/*z* 727). **13** was isolated by column chromatography and fully characterized by ^{1}H/^{13}C/^{31}P NMR spectroscopy, confirming its structure and, indirectly, its parents. The identification of these structures supports the hypothesis of an intramolecular cyclization mechanism of the carbene intermediate **10** with the phosphinoxide.

The peak *m*/*z* 893 is in agreement with **14**, characterized by the two phosphorus set of signals at 76 and 51 ppm in ^{31}P NMR spectra collected in chloroform. This species exists, according to NMR results, both in the open keto- and in the cyclic eno-tautomer **17**, in larger amount in toluene than in chloroform, and comes from a subsequent addition of phosphine to the exocyclic double bond[9] of the phosphorane intermediate. It can further lose ethanol under the MS conditions, giving the **15** (*m*/*z* 847).

Finally, the peak *m*/*z* 757 could represent **16**, formed as a consequence of the loss of ethylene from the phosphorane intermediate **7**, only seen in toluene, due to the instability of the phosphorane intermediate at high temperature.

A summary of MS and ^{31}P NMR data related to each of the species here cited is reported in Table 1. It is worth noting that some extra peaks were detected in ^{31}P NMR spectra. An investigation on the degradation of the starting phosphinoxide was conducted in both chloroform (at 55 °C) and toluene (at 70 °C), leading to the identification of some major derivatives responsible for these extra peaks by means of standard ^{1}H decoupled-^{31}P and ^{1}H coupled-^{31}P NMR, and 2D ^{1}H−^{31}P correlation experiments.

On the basis of this data, the following reaction mechanism is postulated (Scheme 4): from oxalimide **6**, after the addition of phosphine, carbene intermediate **10** and one equivalent of phosphinoxide is formed. Carbene **10** can react with the second equivalent of phosphine, giving the desired phosphorane **7**, or react with the phosphinoxide, leading to impurity **11**. At higher temperatures phosphorane **7** cyclizes to the final trinem ester **8** but can also add another equivalent of phosphine, giving impurity **14** which can lose ethylene to give **15**. Phosphorane **7** itself can lose ethylene, giving impurity **16**. Moreover,

(8) Labaudiniere, L.; Burgada, R. *Tetrahedron* **1986**, *42* (13), 3521.

(9) Castelijns, M. M. C. F.; Schipper, P.; Van Aken, D.; Buck, H. M. *J. Org. Chem.* **1981**, *46* (1), 47.

Table 1. **Summary of MS and ^{31}P NMR data for the step 3 impurities**

product	MS (*m*/*z*)	^{31}P NMR δ (ppm, $CDCl_3$)	^{31}P NMR δ (ppm, toluene-d_8)
$(EtO)_2PMe$ excess	n.a.	175.9[a], 176.2[b]	175.3[a], 175.3[b]
HP(=O)(Me)(OEt)[e]	n.a.	31.3[a], 30.7[b]	27.9[a], 26.5[b]
$(EtO)_2P(=O)Me$[e]	153	28.6[a], 28.3[b]	27.2[a], 26.1[b]
$(EtO)_2P(OMe)$[e]	n.a.	n.d.[a], 137.9[b]	n.d.[a], 136.9[b]
$(HO)_2P(OMe)$[e]	n.a.	n.d.[a], 136.1[b]	n.d.[a], 135.7[b]
HP(=O)$(OEt)_2$[e]	n.a.	n.d.[a], 4.8[b]	n.d.[a,b]
phosphorane **7**	785	75 (various peaks)[a], 75.4 (br.)[b]	76 (various peaks)[a], 75.4[b]
11	801	−28.5[a], −28.3[b]	−29.1[a], −29.5[b]
12	773	n.d.[d]	n.d.[d]
13	727	n.d.[a,b,d], 43.6[c]	n.d.[a], 44.3[b]
14	893.40440[f]	n.d.[a], 75.4, 74.4/52−48 (various peaks)[b]	n.d.[a,b]
15	847.36527[f]	n.d.[d]	n.d.[d]
16	757	n.d.[d]	n.d.[d]
17	893.40440[f]	n.d.[a], 75.4, 74.4/−10, −16 (br.)[b]	n.d.[a], 75.4, 74.7/−11.1, −13.7[b]

[a] Phosphorane **7** formation (spectra collected at 25 °C). [b] Cyclization reaction (spectra collected at 55 °C in $CDCl_3$, 70 °C in toluene-d_8). [c] Isolated material (spectra collected in $CDCl_3$ at 25 °C). [d] Not detected or unclear in the expected chemical shift regions. [e] Degradation products of the starting phosphinoxide identified in a blank reaction in both $CDCl_3$ (at 55 °C) and toluene-d_8 (at 70 °C). [f] Accurate mass measurements carried out using a VG Autospec mass spectrometer, FAB positive ionization mode, and PEG 1000 internal standard. The differences between measured and calculated accurate mass values are ≤5 ppm.

Scheme 4. **Reaction mechanism**

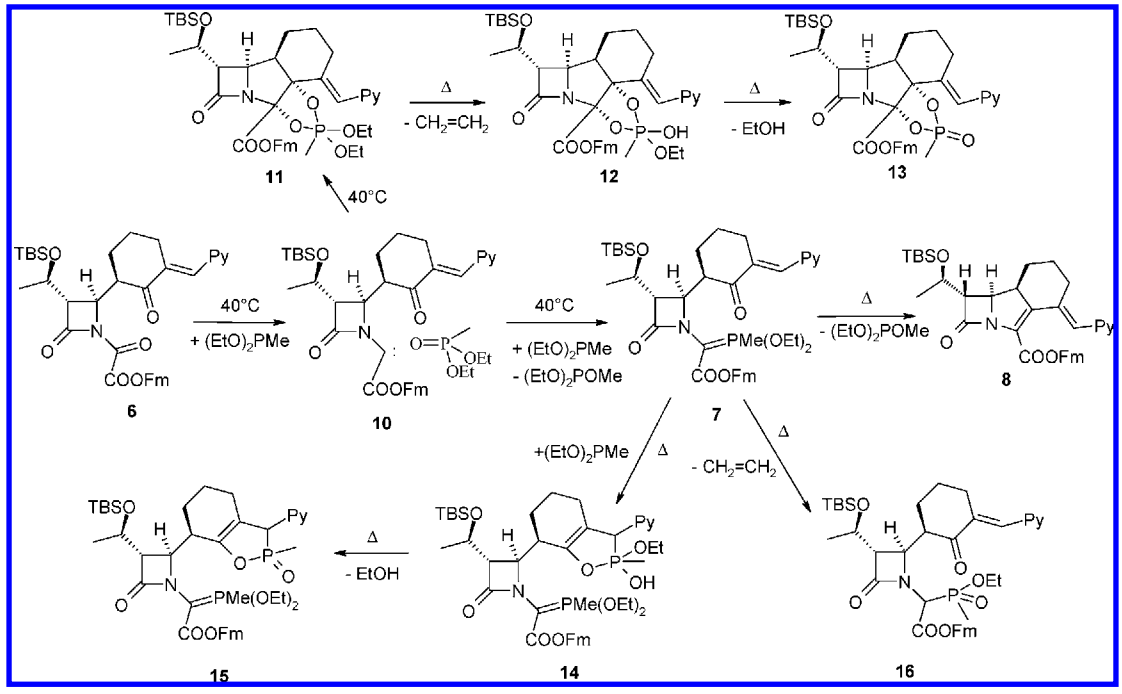

impurity **11** can lose ethylene and ethanol, giving **12** and **13**, respectively. Thus, it appeared that we had a clash between the reaction conditions necessary to prevent the formation of the impurities. In particular, the impurities of the first part of the reaction were due to a competitive reaction of carbene intermediate **10** with the phosphinoxide and the phosphine, and thus, the impurities seemed to be preventable by using an excess of phosphine. However, the impurities of the second part were due to the excess of phosphine and were also solvent dependent: toluene seems to work better in the first part of the reaction and worse in the second, while chloroform works worse in the first part of the reaction and better in the second.

5. Optimization of Step 2b

Having identified the structures of the principal impurities and the cause of their formation, it was possible to devise a new powerful procedure: perform the first part of the reaction in toluene using a large excess of phosphine to reduce the side reactions to **11**, **12**, and **13** and then concentrate the reaction mixture to eliminate toluene and the unreacted phosphine; perform the second part of the reaction in chloroform to reduce the side reactions to **14**, **15**, and **16**, emphasizing the desired pathway.

At this point different DoE studies[10] were performed to optimize the new conditions; in the synthesis of the phosphorane **7** we focused our effort on the optimization of the equivalents of phosphine to be used, volumes of solvent, and temperature. As expected, increasing the equivalents of phosphine resulted in a higher yield in the phosphorane **7** (Figure 7).

(10) The software used for the statistical analysis was Design Expert DX 5. A central composite design (20 experiments with 6 central points) was performed considering phosphine equivalents, concentration, and temperature. As output, the ratio between the HPLC areas of the phosphorane and of naphthalene was considered as the internal standard. The parallel equipment used was SK233 - Anachem.

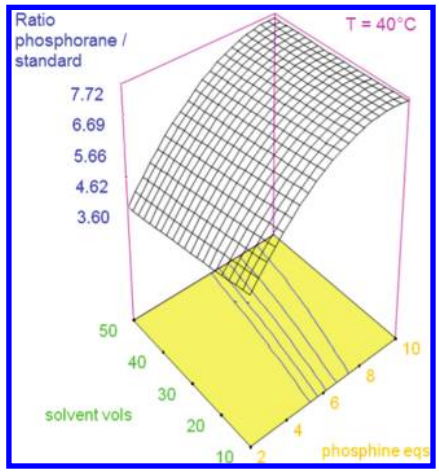

Figure 7. **Phosphorane 7 optimization via DoE.**

Regarding the cyclization, solvent screening was performed to identify a better solvent and substitute for the undesired chloroform.

At the end of the study (Figure 8) the safer cyclohexane/toluene mixture was selected. Applying the above-mentioned conditions, stage 2 global yield reached the target objective (~60%) with a net decrease in the observed impurities.

6. Summary

In this report we described how a combination of NMR and MS analyses made possible not only identifying the structure of the main impurities but also quantifying their amounts. On the basis of these data it was possible to understand the reaction mechanism and to design a better process that matched our target yield.

The final process was successfully scaled up on 10 kg scale and allowed progression to the subsequent clinical studies.

7. Experimental Section

7.1. MS Spectrometry. The reactions were conducted in a reaction vessel directly connected to the electrospray triaxial probe of a Quattro II (Micromass - Waters) mass spectrometer through a fused silica capillary. A positive nitrogen pressure (10 psi) applied to the vessel generated a 2.5 μL/min continuous flow of reaction mixture which entered the ESI probe. An additional makeup solvent (95:5 methanol water at 75 μL/min) was added to the electrospray ionisation (ESI) probe allowing an increase in the ionisation efficiency in positive mode.

7.2. NMR Spectroscopy. ^{31}P NMR spectra were collected using a Varian VXR 300 NMR spectrometer operating at 121.4 MHz. The small-scale reactions were followed directly in 5 mm NMR tubes at controlled operating temperatures in accordance with the effective actual reaction conditions. Both deuterated chloroform ($CDCl_3$) and toluene (toluene-d_8) were used as solvents.

7.3. Synthetic Details. *9H-Fluoren-9-ylmethyl (1S,5E,8aS,8bR)-1-(1-{[(1,1-dimethylethyl)(dimethyl)silyl] oxy}ethyl)-2-oxo-5-(4-pyridinylmethylidene)-1,2,5,6,7,8,8a,8b-octahydroazeto[2,1-a]isoindole-4-carboxylate* ***(8).*** β-Enoneazetidinone oxamate **4** (10 kg, 1 equiv) was suspended in dichloromethane (80 L) at 20 °C, and then aqueous $NaHCO_3$ 4% (80 L) was added. The mixture was stirred, and the aqueous layer was separated and then counterextracted with dichloromethane (25 L). The two organic phases were mixed together and then were concentrated to 50 L. The solution was cooled to 0 °C, DIPEA (6.78 L, 2 equiv) was added, and then a solution of FmOCOCOCl **7** (8.52 kg, 1.5 equiv) in dichloromethane (5 L) was added in 30 min. Toluene (110 L) was added 15 min after the end of the addition; then the solution was washed with aqueous NaCl 10% (80 L), and the organic solution of **6** was then dried via azeotropic distillation. To this solution was added $(EtO)_2PMe$ (50% in iso-octane, 18 L, 3 equiv), and this mixture stirred at 30 °C for 50 min and was then concentrated under vacuum to about 30 L. Cyclohexane (300 L) was added and the mixture heated at 90 °C for 70 min and then cooled to 20 °C. The solution was filtered through an alumina pad (20 kg), the pad was washed

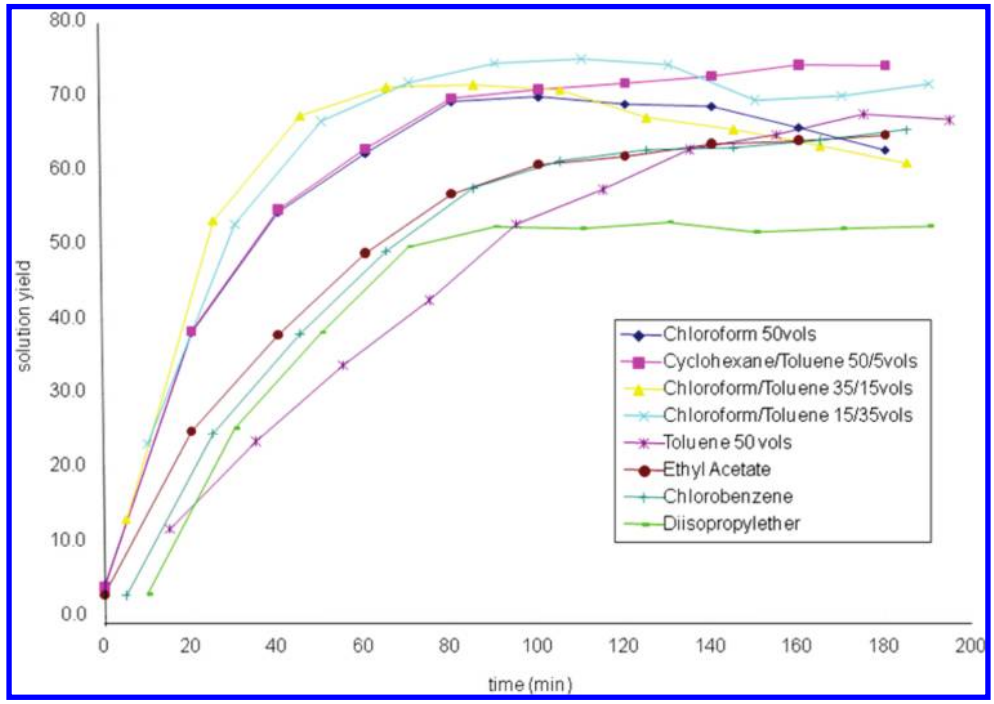

Figure 8. **Screening of solvents for the cyclization to 8.**

with toluene (2 × 30 L), and the organics were concentrated to 20 L. Di-isopropyl ether (82 L) was added in 30 min and the suspension cooled to 0 °C for 1 h. The suspension was filtered, and the solid obtained was washed with cold di-isopropyl ether (16.5 L) and dried at 40 °C under vacuum, yielding **8** (7.5 kg, 60%).

^{1}H NMR (500 MHz, $CDCl_3$): δ 0.12 (s, 3H); 0.13 (s, 3H); 0.93 (s, 9H); 1.27 (d, J = 6.3 Hz, 3H); 1.60−1.50 (m, 2H); 2.10−1.95 (m, 2H); 2.22 (m, 1H); 3.02 (m, 1H); 3.12 (m, 1H); 3.37 (dd, J = 5.9, 3.0 Hz, 1H); 4.26 (m, 1H); 4.30 (m, 1H); 4.40 (m, 2H); 4.50 (m, 1H); 6.44 (m, 1H); 7.07 (d, J = 6.6 Hz, 2H); 7.28 (m, 2H); 7.39 (m, 2H); 7.63 (d, J = 7.0 Hz, 1H); 7.72 (d, J = 7.0 Hz, 1H); 7.75 (m, 2H); 7.82 (d, J = 6.6 Hz, 2H).

Acknowledgment

We thank Damiano Papini for the HPLC analytical support, Carla Marchioro for the valuable NMR discussion, Tino Rossi, Gilberto Vigelli, and Pieter Westerduin for their useful suggestions.

Received for review April 12, 2010.

OP100097C